Initial Atomic Motion Immediately Following Femtosecond-Laser Excitation in Phase-Change Materials

E. Matsubara,[1,*] S. Okada,[1] T. Ichitsubo,[1,†] T. Kawaguchi,[2] A. Hirata,[3,4] P. F. Guan,[5] K. Tokuda,[1] K. Tanimura,[6] T. Matsunaga,[2] M. W. Chen,[3,7] and N. Yamada[1,‡]

[1]*Department of Materials Science and Engineering, Kyoto University, Kyoto 606-8501, Japan*
[2]*Office of Society-Academia Collaboration for Innovation, Kyoto University, Kyoto 611-0011, Japan*
[3]*WPI Advanced Institute for Materials Research, Tohoku University, Sendai 980-8577, Japan*
[4]*Mathematics for Advanced Materials-OIL, AIST-Tohoku University, Sendai 980-8577, Japan*
[5]*Beijing Computational Science Research Center , Beijing 100084, People's Republic of China*
[6]*The Institute of Scientific and Industrial Research, Osaka University, Osaka 567-0047, Japan*
[7]*State Key Laboratory of Metal Matrix Composites, School of Materials Science and Engineering, Shanghai Jiao Tong University, Shanghai 200030, People's Republic of China*

(Received 21 June 2016; published 21 September 2016)

Despite the fact that phase-change materials are widely used for data storage, no consensus exists on the unique mechanism of their ultrafast phase change and its accompanied large and rapid optical change. By using the pump-probe observation method combining a femtosecond optical laser and an x-ray free-electron laser, we substantiate experimentally that, in both GeTe and $Ge_2Sb_2Te_5$ crystals, rattling motion of mainly Ge atoms takes place with keeping the off-center position just after femtosecond-optical-laser irradiation, which eventually leads to a higher symmetry or disordered state. This very initial rattling motion in the undistorted lattice can be related to instantaneous optical change due to the loss of resonant bonding that characterizes GeTe-based phase change materials. Based on the amorphous structure derived by first-principles molecular dynamics simulation, we infer a plausible ultrafast amorphization mechanism via nonmelting.

DOI: 10.1103/PhysRevLett.117.135501

The ultrafast response of phase-change materials (PCMs) under short-pulse excitation has now attracted strong attention from both basic and applied research [1,2]. Based on large physical-property differences exhibited by their crystalline and amorphous structural phases and based on fast rates of crystallization and amorphization, PCMs are now widely used as active media in data storage devices; the most typical material is the rocksalt $Ge_2Sb_2Te_5$ (GST)[3]. The phase change in the GST family (pseudobinary system of GeTe-Sb_2Te_3), including rocksalt $Ge_2Sb_2Te_5$ and trigonal-rhombohedral GeTe, can be induced by the irradiation of nanosecond (ns)-laser pulse [4–7]. Instead of ns-laser pulses that induce phase changes in thermal mechanisms, fs- and ps-laser pulses have been used to induce faster operating speeds [8,9], together with utilizing possible electronic effects specific to short-pulse excitation [10].

PCMs are essentially IV-VI compounds, and electronic structures are characterized as the half-filled *p*-type bonds aligning in their crystalline phases. The *p*-type bonds involve two inherently competing stabilization mechanisms: resonant bonding [11,12] and Peierls distortion [13]. As a result, all PCMs have distorted cubic structures; Ge-Te bonds split into the short and long bonds. In the crystalline phase, Ge atoms are sixfold coordinated, while they are mostly distorted and fourfold coordinated in amorphous phases [13,14]. Therefore, the local structure of Ge atoms relative to Te sites, together with the long-range order, is the central issue in understanding the electronic and structural properties of PCMs. This issue becomes more critical under short-pulse excitation, as photoinduced electronic-order changes induce strong modifications of the atomic potentials to stimulate coherent-phonon generation [15] and local structural changes, which are related to transformation into other phases.

In order to capture directly the structural changes of PCMs under short-pulse excitation, an ultrafast electron diffraction (UED) technique has been applied extensively. Hada *et al.* [16] have concluded that umbrella-flip motions of Ge atoms, where rhombohedral distortion is enhanced, is responsible for the structural changes in the laser excitation of GST. In contrast, Hu *et al.* [17] have concluded that rhombohedral distortion of Ge atoms is reduced to transiently attain the cubic structures of GeTe. Thus completely opposite conclusions have been drawn in previous UED works, leaving the initial structural change unsolved in fs-laser excited GeTe-based PCMs.

Unambiguous elucidation of local structural changes in a unit cell of PCMs at the atomic level needs precisely resolving the lowest-index diffraction lines, 003/101 in rhombohedral GeTe and 111 in rocksalt GST, and tracing their changes at ps-temporal regime. Unfortunately, UED experiments have drawbacks of low scattering-angle resolution and of ambiguous diffraction-intensity changes due to the dynamical effects of scattering. In this Letter, we

overcome these drawbacks of UED applying time-resolved x-ray diffraction to resolve low-index diffraction peaks, and present a precise picture of the initial laser-induced motions of Ge atoms in the Te sublattice of GeTe and GST. Furthermore, with the aid of the first-principles molecular dynamics simulation, based on the amorphous structure of GST, we discuss the amorphization mechanism in PCMs.

To this goal, we employed the x-ray free-electron laser (XFEL) at SACLA in Japan [18], which combines both high intensity and an ultrashort pulse width for "femtosecond XRPD" (fs-XRPD) [19,20]. In order to detect the very initial atomic motion immediately following fs-laser irradiation, we conducted repeated pump-probe measurement in the "reversible regime," where the irreversible structure change from crystal to amorphous was prohibited to accumulate the diffraction intensities for high accuracy. The fs-XRPD (probe) spectrum was monitored by the 2D detector at every time delay, τ, after the fs-laser (pump) irradiation of the 800-nm wavelength with a pulse width of 30 fs, whose photon energy (~1.5 eV) is sufficiently higher than the band gap (~0.5 eV) of GST materials [21]. The detailed pump-probe procedure is described in the Supplemental Material (see Fig. S1) [22].

Figure 1(a) shows the time-resolved fs-XRPD spectra monitored for trigonal-rhombohedral GeTe, where the spectra were detected in the transmission geometry. The GeTe crystal has a unidirectional Peierls distortion along the [001] direction (corresponding to the [111] direction in the cubic system) [25], while the $Ge_2Sb_2Te_5$ crystal possesses eight equivalent Peierls distortions along the $\langle 111 \rangle$ directions; the former is called the ordered state, and the latter is called the disordered state [26,27]. In the present pump-probe experiment, the time zero ($\tau = 0$) was assigned as the time when the derivative of the 200 intensity with regard to time starts to decrease, this being reasonable in light of the electron-beam-diffraction studies [16,28]. As clearly shown in the fs-XRPD profiles in Fig. 1(a), the peak position of the 012 line remains constant, but intensities of 003 and 110 peaks change dramatically within 4 picoseconds after excitation. Around 26 picoseconds, the trigonal-rhombohedral crystal of GeTe appears to be changed transiently to a cubiclike crystal, as two sets of the split diffraction peaks (003/101 and 104/110) clearly merge into single peaks (the former and latter sets correspond to 111 and 220 in cubic system, respectively), associated with volume expansion; the 012 peak (corresponding to 200 in cubic system) shifts to lower scattering vector side. The experimental fact that the diffraction intensities change while keeping the lattice symmetry (within 4 picoseconds) reveals that the barycenter of the Ge-Te structural motif remains but the motif itself varies just after fs-laser irradiation. The selective loss of diffraction intensities of the 003 and 110 peaks, while keeping those of the 101 and 104 peaks essentially unchanged, is the key to understanding the motif changes.

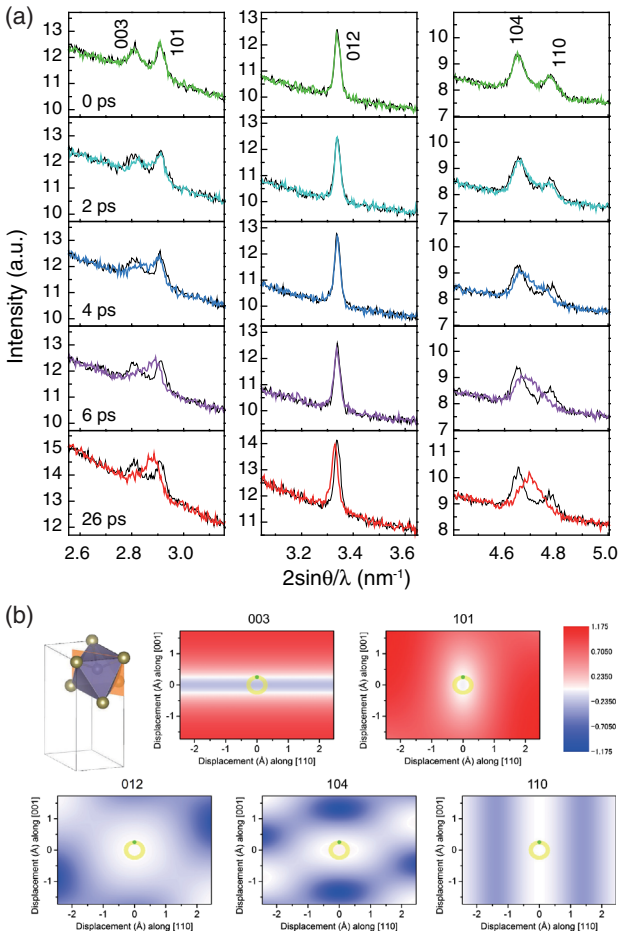

FIG. 1. (a) Time-resolved fs-XRPD spectra just after fs-laser irradiation obtained for GeTe (black lines behind color lines are the x-ray diffraction spectra obtained at off-laser state, i.e., indicating I_0). The measurements were conducted in the transmission geometry. (b) Square of structure factors as a function of Ge position in the rhombohedral GeTe. The values of $\log(I/I_o)$ are drawn in the maps, where I_o denotes the intensity at the original Ge position (green point).

In order to account for this, we have calculated the structure factor as a function of the relative position of the Ge atom from the fixed Te position. This is reasonable in light of the recent first-principles molecular dynamics calculation [10], which shows that electronic excitation induces selective effects on Ge atoms in GST. In addition, this is also supported the resulted amorphous structure discussed later (Fig. 5). The detailed calculation procedure is described in the Supplemental Material (see Figs. S3–S5) [22]. Figure 1(b) shows maps of the square of the structure factors (i.e., intensity maps), which show a trajectory of the atomic motion of Ge in the ultrafast time region that can satisfy the experimental trend in the intensity changes. As found from Fig. 2(a), the 003 structure factor increases if the Ge atom moves further along the [001] direction (i.e., along the c axis), which does not reflect the experimental structure factor. Since the 012 intensity remains unchanged

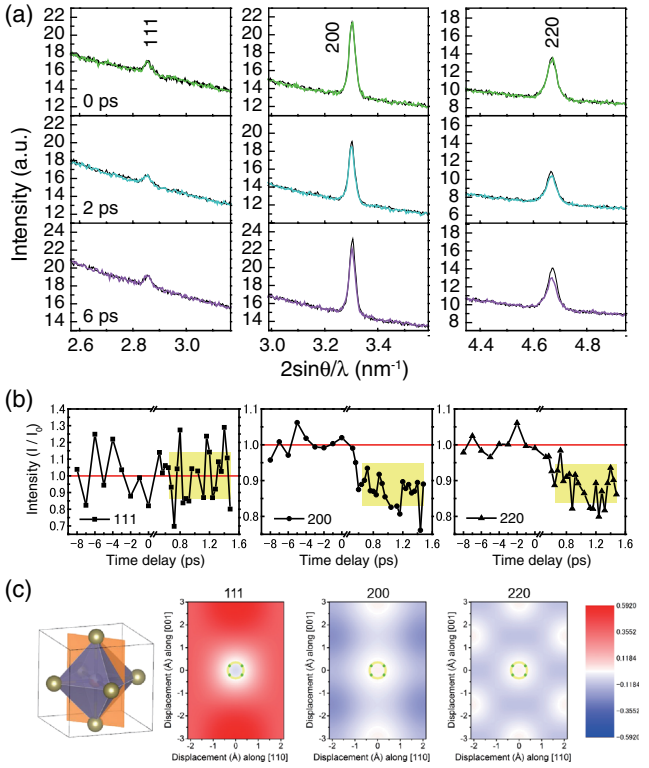

FIG. 2. (a) Time-resolved fs-XRPD spectra just after fs-laser irradiation obtained for $Ge_2Sb_2Te_5$ (black lines behind color lines indicate I_0). (b) Time-dependent peak intensities of the diffraction peaks (111, 200, 220) in the very early time region measured for $Ge_2Sb_2Te_5$, where the yellow regions represent the averages with the standard deviations. The abrupt decreases of the 200 and 220 diffractions occur within about 400 fs, and their overall decays are characterized by a time constant of about 8 ps. (c) Square of structure factors as a function of Ge position in $Ge_2Sb_2Te_5$, where the DW-factor change is taken into account in this case. Since the values of $\log(I_{cal}/I_{exp})$ are drawn, the white regions showing $\log(I_{cal}/I_{exp}) \approx 0$ indicate the Ge positions that satisfy the experimental intensities, where I_{exp} is the representative value in the yellow regions in (b).

experimentally, it is expected that the trajectory of the Ge motion is on the contour like a circle (around the center position, not on the center) drawn in the 012 intensity map in Fig. 2(a). As found from all the structure-factor maps, when the Ge atom is located at any point on (or moves along) the circle, the changes in the intensities calculated for the five diffractions substantially satisfy the experimental intensity changes (012: almost unchanged, 003 and 110: significant decrease, 101 and 104: slight change) in Fig. 1(b). It is worthwhile to note that, if on-centering of the Ge atom occurs, the 110 intensity should remain unchanged, but actually the intensity significantly drops down. This indicates that the fs-laser-excited Ge atoms do not move further away along the [001] direction (corresponding to [111] in cubic system), but rather they move "around the center position" with keeping off-center, leading to a higher crystal symmetry. We call this "rattling motion." The present accurate and precise fs-XRPD analysis can allow us to conduct the accurate analysis based on the time-resolved diffraction intensities, and the present interpretation is beyond the ambiguous discussion from the electron diffraction intensity.

A similar phenomenon occurs also in the $Ge_2Sb_2Te_5$ crystal. As seen in Figs. 2(a) and 2(b), the intensities of the 200 and 220 diffractions significantly decrease, while that of the 111 diffraction is substantially unchanged (see Fig. S2 for details in the Supplemental Material). The most advantageous point in this work is that we can successfully monitor the time-dependent intensity of the 111 superlattice diffraction, which is key for discussing the Ge-atom position or movement, but this was not mentioned in the previous studies [16,28]. As well as in the case of GeTe, the rattling motion of Ge (and also Sb) atoms would take place in the undistorted lattice. However, for $Ge_2Sb_2Te_5$, it is slightly complicated to understand the experimental behavior, because we cannot discuss merely on the basis of the crystal symmetry change like GeTe. In this case, to discuss more quantitatively, we need to take account of the enlargement in the Debye-Waller (DW) factor [22]. As well as GeTe, we have calculated the site-dependent structure factors for $Ge_2Sb_2Te_5$; see the Supplemental Material for details (see Figs. S3, S4). In Fig. 2(c), similarly the yellow circles in the maps indicate a trajectory of the atomic motion of Ge that simultaneously fulfills the experimental intensity changes in the 111, 200, and 220 diffractions in Fig. 2(b). It should be noted that the movement of Ge atoms along [111] leads to drastic increase in the intensity of the 111 diffraction as seen in Fig. 2(b) and also in Fig. S3 in the Supplemental Material, but it remains experimentally unchanged as seen in Fig. 2(a) and 2(b). Thus, also in this case, the Ge atom off-centered along the [111] direction cannot move further along the [111] direction, which is clearly in contrast to the typical motion of Ge in the umbrella-flip model, at least, in such a very early time region.

Based on the present experimental results and analyses, Fig. 3(a) schematically illustrates the "rattling motion" in the lattice weakened by the laser stimulation, and Figs. 3(b) and 3(c) illustrate the relation between the atomic motion, lattice symmetry and DW-factor change, for GeTe and $Ge_2Sb_2Te_5$, respectively. As is discussed in the review paper, Ref. [29], the lattice can be weakened by the laser-excited electrons from bonding states to antibonding states, even when the lattice is still "cold." Incidentally, it was recently reported that GST lattice remains cold for 4 picoseconds for GST [30]. The weakened lattice has softer elastic constants, and the curvature of the potential becomes shallower, by which the position of Ge atoms would be able to shift rather freely with changing the Ge-Te bond lengths in the laser-excited state, and consequently the Ge atoms in GeTe or GST have a capability of rattling motion by the laser stimulation. By the rattling motion of Ge, the

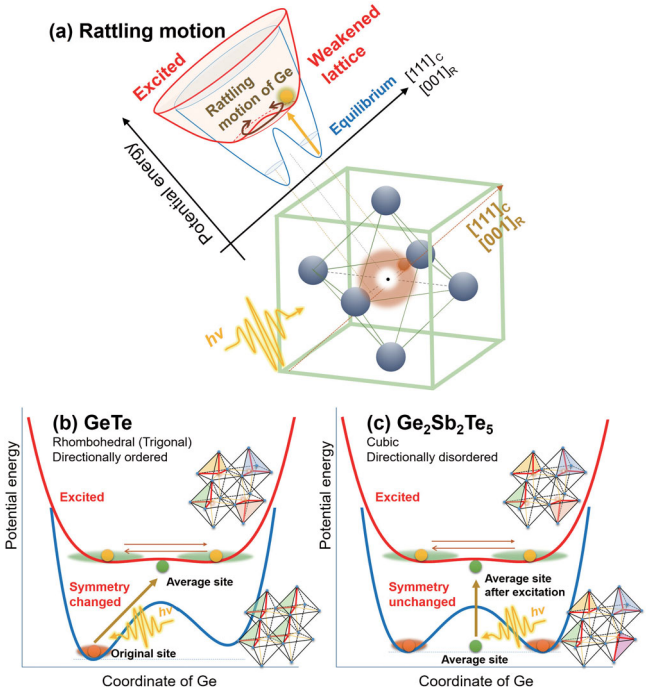

FIG. 3. Schematic illustration of (a) the rattling motion of Ge in the Ge-Te structural motifs and (b) and (c) the transient structural transformation induced by the rattling motion of Ge in for GeTe and in for $Ge_2Sb_2Te_5$. In both cases, Ge atoms move so as to circumvent the central position of the octahedron consisting of Te atoms.

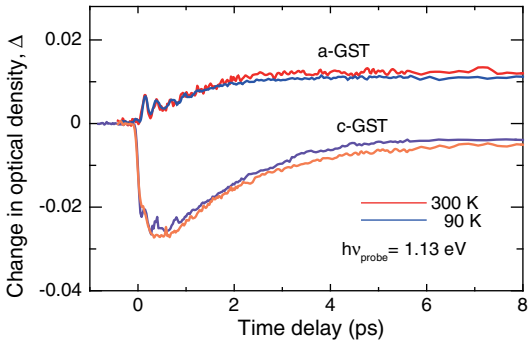

FIG. 4. The change in the optical density after the pump for the two phases, rocksalt $Ge_2Sb_2Te_5$ (c-GST) and amorphous $Ge_2Sb_2Te_5$ (a-GST). The pump energy is 1.55 eV and the probe energy is 1.13 eV in the present pump-probe measurement. To consider the phonon effect, the measurement was conducted also at 90 K in addition to 300 K. The oscillatory features just after the pump pulse in a-GST can be attributed to coherent generation of LO phonons related to Ge-Te bonds (Ref. [15]). The structure is enhanced strongly in a-GST; corresponding structures in c-GST are very weak. The initial decrease of optical density (300 K) is characterized by a time constant of 130 fs, while the partial recovery till 6 ps is characterized by the constant of 1.9 ps.

rhombohedral GeTe lattice tends to change to a cubic lattice, as shown in Fig. 3(b). On the other hand, since the rocksalt $Ge_2Sb_2Te_5$ crystal has a random Peierls distortion, as seen in Fig. 3(c), x ray sees that it behaves as a cubic crystal whose Ge atoms are located at the average (center) sites. After the laser stimulation, the lattice is weakened to make the potential energy shallow and the position of the excited Ge atoms becomes unfixed in the wide range, thus increasing the DW factor of Ge atoms.

A very recent paper on the electron-diffraction pump probe for GeTe [17] is worthwhile as the first recognition of the movement to the center position, suggesting a model different from the "umbrella-flip" model [13]. In their electron diffraction data, differently from the present data, the 003/101 diffractions and the 104/110 diffractions could not be separated due to the common problem in the low scattering-angle resolution, which inhibits quantitative analysis as presented here. In contrast, the present precise x-ray diffraction (XRD) data enabled us to analyze the trajectory of Ge (or Te) atoms for both GeTe and $Ge_2Sb_2Te_5$ crystals, which shows that, in both cases, the rattling motion of Ge (or Te) atoms takes place "circumventing" the center position. The rattling motion around the center revealed here and simple on-centering motion in Ref. [17] give critically different effects on optical properties of PCMs. In the case of the on-centering of the Ge (or Te) atom, the resonant bonding is considered to be further enhanced [12], which leads to the increase of the real part of dielectric function, leading to the increase in optical absorbance. However, the optical density (or absorbance) actually decreases very rapidly while the lattice remains cold. Figure 4 shows the change in optical density after the pump, Δ, for the two phases, rocksalt GST and amorphous GST. Actually, it is clearly seen that Δ for c-GST largely decreases within 500 femtoseconds, while that for a-GST substantially increases. This strongly suggests that the resonant bonding in c-GST is lost just after fs-laser irradiation. Recently, Waldecker *et al.* [28] also clarified that a drastic change in the dielectric function by the loss of resonant bonding can take place even in a time domain where the lattice is still cold (within 0.1-2 picoseconds). The rattling motion prior to lattice distortion presented here can reasonably explain such an instantaneous loss of resonant bonding, because Ge (or Te) atoms move "around" the center position, and then the necessary condition for the resonant bonding (i.e., the *p* orbital's alignment) is inevitably lost.

The rattling motion may have a strong implication to the amorphization that takes place at the high excitation-density regime, as discussed below based on the first-principles molecular dynamics (FPMD) simulation [31–34] with the Voronoi polyhedral analysis; see also the procedure described in the Supplemental Material. Detailed results with angstrom-beam electron diffraction analysis will appear elsewhere. Figure 5(a) shows that populations of the Voronoi octahedral coordinate [Fig. 5(b)] around Ge/Sb are much higher than that of Te. This strongly indicates that the Te frame is substantially rigid rather than the Ge/Sb

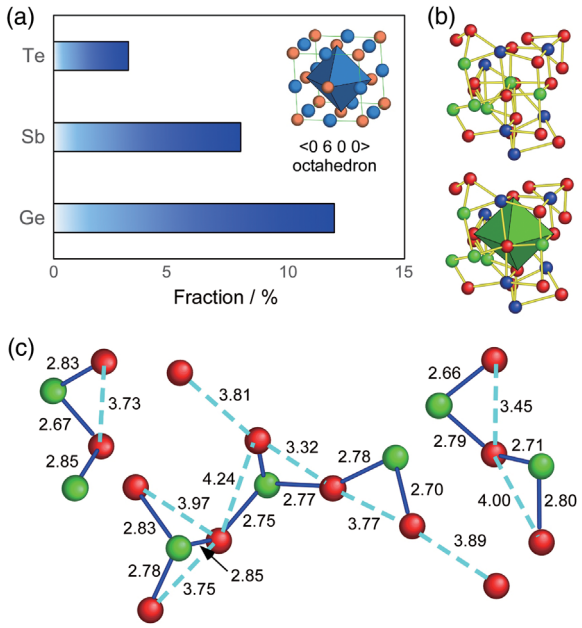

FIG. 5. FPMD simulation with Voronoi polyhedral analysis for a-GST (Ge:50, Sb: 50, Te: 125 atoms). (a) Population of the octahedral cluster $\langle 0600 \rangle$ around each atom in a-GST. (b) Typical octahedral cluster around Ge atom. Green, blue, and red circles denote Ge, Sb, and Te atoms, respectively. (c) Linear-like Te chain in amorphous GST. The unit of the bond length is angstrom.

frame, consistent with the previous work by XRD with reverse Monte Carlo analysis [35]. Raty *et al.*[25] have shown that even the cluster in liquid of GeTe possesses a certain kind of Peierls distortion, which suggests that substances showing Peierls distortion in the solid state tend to dimerize in the liquid state. As shown in Fig. 5(c), since the connection of Te is rather a one-dimensional linearlike chain (or like long molecules), Peierls-like dimerization appears to dominate in the amorphous state, in that most of the Te-Ge bond lengths are shorter than the shorter-bond length (~2.83 Å) in the rocksalt crystal. Originally, the concepts of resonant bonding and Peierls distortion were competing each other, and hence, in our opinion, the resonant bonding would be dominated in the crystal (where Ge atoms play a role of glue between Te linear chains), while Te-Ge dimers would be favored in the amorphous state where the resonant bonding is lost, which is supported by the optical property shown in Fig. 4. Thus, it is expected that, after fs-laser irradiation, the high excitation-density regime (i.e., more active or more numerous rattling motions of Ge atoms in the crystals) induces destruction of resonant bonding state, and consequently Peierls-like dimerization precedes the weakened resonant bonding. Thus, photoexcitation triggers switching of the bonding nature from resonant bonding to Peierls-like dimerization due to the rattling motion, and thereby the amorphous state would be induced via nonmelting at a high excitation-density regime. This scenario is also supported by the FPMD study by Li *et al.* [10] and by Huang-Robertson's amorphous picture [14].

In summary, this work presents a crucial picture of the initial motion for the ultrafast phase-change mechanism of GST alloys. The rattling motion of mainly Ge atoms takes place just after fs-laser irradiation, and thereby the resonant bonding is lost, which can be a trigger of the lattice-symmetry change, disordering, and eventual amorphization. Thus, this rattling motion of Ge would be a key for consideration of all the phase change processes in the GeTe-based phase change materials.

We would like to thank Professor Y. Tanaka, Dr. M. Yabashi, and all the staff scientists, Dr. K. Ogawa, and Dr. S. Owada at SACLA for maintaining the high performance of the XFEL throughout our experiments. We are deeply indebted to Dr. R. Kojima, Mr. K. Kawahara, Mr. A. Tsuchino, and Dr. K. Nishiuchi (Panasonic) for their great assistance in the sample preparations. The experiments at SACLA were performed at the BL3 of SACLA with the approval of the Japan Synchrotron Radiation Research Institute (JASRI) (Proposals No. 2012B8044, No. 2013A8048, No. 2013B8053, No. 2014A8037, and No. 2014B8062). This work was supported by the X-ray Free Electron Laser Priority Strategy Program (MEXT).

*matsubara.eiichiro.6z@kyoto-u.ac.jp
†tichi@mtl.kyoto-u.ac.jp
‡yamada.noboru.4z@kyoto-u.ac.jp

[1] S. R. Ovshinsky, Phys. Rev. Lett. **21**, 1450 (1968).
[2] J. Feinleib, J. deNeufville, S. C. Moss, and S. R. Ovshinsky, Appl. Phys. Lett. **18**, 254 (1971).
[3] N. Yamada, E. Ohno, N. Akahira, K. Nishiuchi, K. Nagata, and M. Takao, Jpn. J. Appl. Phys. **26**, 61 (1987).
[4] M. Chen, K. A. Rubin, and R. W. Barton, Appl. Phys. Lett. **49**, 502 (1986).
[5] N. Yamada, E. Ohno, K. Nishiuchi, N. Akahira, and M. Takao, J. Appl. Phys. **69**, 2849 (1991).
[6] N. Yamada, Phys. Status Solidi B **249**, 1837 (2012).
[7] M. Wuttig and N. Yamada, Nat. Mater. **6**, 824 (2007).
[8] M. Konishi, H. Santo, Y. Hongo, K. Tajima, M. Hosoi, and T. Saiki, Appl. Opt. **49**, 3470 (2010).
[9] A. Kolobov, P. Fons, M. Krbal, and J. Tominaga, J. Non-Cryst. Solids **358**, 2398 (2012).
[10] X. B. Li, X. Q. Liu, X. Liu, D. Han, Z. Zhang, X. D. Han, H. B. Sun, and S. B. Zhang, Phys. Rev. Lett. **107**, 015501 (2011).
[11] G. Lucovsky and R. M. White, Phys. Rev. B **8**, 660 (1973).
[12] K. Shportko, S. Kremers, M. Woda, D. Lencer, J. Robertson, and M. Wuttig, Nat. Mater. **7**, 653 (2008).
[13] A. V. Kolobov, P. Fons, A. I. Frenkel, A. L. Ankudinov, J. Tominaga, and T. Uruga, Nat. Mater. **3**, 703 (2004).
[14] B. Huang and J. Robertson, Phys. Rev. B **81**, 081204 (2010).
[15] M. Hase, P. Fons, K. Mitrofanov, A. V. Kolobov, and J. Tominaga, Nat. Commun. **6**, 8367 (2015).

[16] M. Hada, W. Oba, M. Kuwahara, I. Katayama, T. Saiki, J. Takeda, and K. G. Nakamura, Sci. Rep. **5**, 13530 (2015).
[17] J. Hu, G. M. Vanacore, Z. Yang, X. Miao, and A. H. Zewail, ACS Nano **9**, 6728 (2015).
[18] H. Tanaka *et al.*, Nat. Photonics **6**, 540 (2012).
[19] A. Cavalleri, C. Tóth, C. W. Siders, J. A. Squier, F. Ráksi, P. Forget, and J. C. Kieffer, Phys. Rev. Lett. **87**, 237401 (2001).
[20] K. Sokolowski-Tinten, C. Blome, J. Blums, A. Cavalleri, C. Dietrich, A. Tarasevitch, I. Uschmann, E. Förster, M. Kammler, M. Horn-von-Hoegen, and D. Linde, Nature (London) **422**, 287 (2003).
[21] T. Kato and K. Tanaka, Jpn. J. Appl. Phys. **44**, 7340 (2005).
[22] See Supplemental Material at http://link.aps.org/supplemental/10.1103/PhysRevLett.117.135501, which includes Refs. [23, 24], for the details of the structure factor calculation considering the Debye-Waller factors.
[23] P. B. Pereira, I. Sergueev, S. Gorsse, J. Dadda, E. Muller, and R. P. Hermann, Phys. Status Solidi B **250**, 1300 (2013).
[24] T. Matsunaga, N. Yamada, and Y. Kubota, Acta Crystallogr. Sect. B **B60**, 685 (2004).
[25] J. Y. Raty, V. Godlevsky, P. Ghosez, C. Bichara, J. P. Gaspard, and J. R. Chelikowsky, Phys. Rev. Lett. **85**, 1950 (2000).
[26] M. Krbal, A. V. Kolobov, P. Fons, R. E. Simpson, T. Matsunaga, J. Tominaga, and N. Yamada, Phys. Rev. B **84**, 104106 (2011).
[27] T. Matsunaga, P. Fons, A. V. Kolobov, J. Tominaga, and N. Yamada, Appl. Phys. Lett. **99**, 231907 (2011).
[28] L. Waldecker, T. Miller, M. Rude, R. Bertoni, J. Osmond, V. Pruneri, R. E. Simpson, R. Ernstorfer, and S. Wall, Nat. Mater. **14**, 991 (2015).
[29] S. K. Sundaram and E. Mazur, Nat. Mater. **1**, 217 (2002).
[30] K. V. Mitrofanov *et al.*, Sci. Rep. **6**, 20633 (2016).
[31] G. Kresse and J. Furthmuller, Comput. Mater. Sci. **6**, 15 (1996).
[32] M. P. Allen and D. J. Tidesley, *Computer Simulation of Liquids* (Oxford University Press, New York, 1987).
[33] P. E. Blochl, Phys. Rev. B **50**, 17953 (1994).
[34] Y. Wang and J. P. Perdew, Phys. Rev. B **44**, 13298 (1991).
[35] J. Akola, R. O. Jones, S Kohara, S. Kimura, K. Kobayashi, M. Takata, T. Matsunaga, R. Kojima, and N. Yamada, Phys. Rev. B **80**, 020201 (2009).